Applied Energy 333 (2023) 120576

Contents lists available at ScienceDirect

Applied Energy

journal homepage: www.elsevier.com/locate/apenergy

Energy storage performance improvement of phase change materials-based triplex-tube heat exchanger (TTHX) using liquid–solid interface-informed fin configurations

Ben Palmer [a], Adeel Arshad [b], Yan Yang [a,*], Chuang Wen [a,*]

[a] Faculty of Environment, Science and Economy, University of Exeter, Exeter EX4 4QF, United Kingdom
[b] Environment and Sustainability Institute (ESI), University of Exeter, Penryn Campus, Penryn, Cornwall TR10 9FE, United Kingdom

HIGHLIGHTS

- Fluid-solid interface-informed fin configuration to enhance phase change material performance.
- Natural convection of melting process of phase change materials is considered in the simulations.
- Efficient melting performance is achieved in tubular thermal energy storage systems.
- Charging performance is improved by 57.4 % using fluid-solid interface-informed fin configurations.

ARTICLE INFO

Keywords:
Energy storage
Phase change material
Melting process
Heat exchanger
Fin configuration
Computational fluid dynamics

ABSTRACT

The future of power generation is predicted to be greener with greater uptake in renewable energy which will be more intermittent and make matching demand harder. Latent thermal energy storage using phase change materials (PCMs) could provide a solution to that problem. PCMs can store large amounts of energy in small volumes, however, the main issue is the low conductivity of PCMs, which limits the rate that energy can be stored due to the slow melting and solidification processes. In the present study, we design and optimise a flow structure-informed fin configuration for triplex-tube heat exchangers (TTHXs) that accelerates the PCM melting process to allow for faster energy storage rates. The computational fluid dynamics modelling is developed to evaluate different TTHX geometries and find the most efficient fin geometries. The results show that an optimal fin geometry can provide a 57.4 % reduction in melting time, which demonstrates that fins offer a very effective way of reducing the melting times of PCMs without taking up much volume. We also found that fins in the lower half of the PCM are more effective in reducing total melt time than fins in the upper half. It is revealed that curved fins offer better performance when compared to similar straight fins. Lastly, it is observed that horizontal or angled surfaces allow for more natural convection in TTHX. The findings can be used to inform future studies on energy storage performance improvement of PCMs.

1. Introduction

The integration of solar energy into heating and cooling systems is an efficient way to provide greener energy while reducing carbon emissions. Thermal energy storage could improve the flexibility of the solar-based heating and cooling system due to the intermittent nature of solar energy. Phase change materials (PCMs) are materials which store and release large amounts of energy as they change state, and this characteristic can be utilised for various applications such as energy storage and thermal comfort control [1–3]. Utilising PCMs efficiently and improving performance is an evolving area of study with many potential applications. Due to global warming, there is a growing need to reduce emissions in the built environment sector because buildings and construction account for 39 % of annual global CO_2 emissions [4]. Some innovations in the built environment include PCM insulation and energy storage solutions [5–7]. PCM insulation helps reduce the energy demand of a building and therefore emissions by storing excess thermal energy and releasing it when needed [8–9]. This helps maintain thermal comfort for the building occupants which will is important especially as the

* Corresponding authors.
E-mail addresses: yanyang2021@outlook.com (Y. Yang), c.wen@exeter.ac.uk (C. Wen).

https://doi.org/10.1016/j.apenergy.2022.120576
Received 3 August 2022; Received in revised form 10 December 2022; Accepted 23 December 2022
Available online 30 December 2022
0306-2619/© 2022 The Author(s). Published by Elsevier Ltd. This is an open access article under the CC BY license (http://creativecommons.org/licenses/by/4.0/).

Nomenclature

PCM	Phase Change Material
TTHX	Triplex-tube Heat Exchanger
TES	Thermal Energy Storage
LHS	Latent Heat Storage
SHS	Sensible Heat Storage
HTF	Heat Transfer Fluid
G	Latent Heat of fusion (kJ/kg)
ρ	Density (kg/m^3)
C_p	Specific heat (J/kg K)
k	Heat expansion coefficient (W/m K)
μ	Dynamic viscosity (kg/ms)
T_s	Solidus temperature (K)
T_l	Liquidus temperature (K)
β	Thermal Expansion Coefficient (K^{-1})
λ	Liquid Fraction
ε	Small parameter to avoid dividing by zero
θ	Tangent angular direction
C	Mushy zone constant
S	Source term
t	Time (s)
g	Acceleration due to gravity (m/s^2)
P	Pressure (Pa)
u	Velocity in the r-direction
v	Velocity in the θ-direction
r	Radial direction

climate becomes more extreme. The need for energy storage will also be increasing in the future as clean power generation sources such as renewables become much more prevalent to meet the Paris Agreement goals. As a result of renewables' varying and unpredictable nature, some form of energy storage will be needed to help demand match the varying supply. Latent heat storage units using PCM technology to store heat could be a space-efficient method of achieving this [10].

One of the reasons why PCMs have not been widely adopted in energy storage applications is that they often have low thermal conductivities [11–12]. This limits their usefulness because the charging and discharging times are too long for most applications [13–14]. To combat this drawback various methods have been used such as metal foam [15–16], nanoparticles [17–19] and fins [20–22]. Nanoparticle dispersion in PCMs was first numerically investigated by Khodadadi and Hosseinizadeh [23] and was shown to improve thermal conductivity which is beneficial for thermal energy storage (TES) applications. Research on nanoparticles in PCMs enclosed in a TTHX has been conducted by Mahdi et al. [24] and the results showed that nanoparticles can provide up to a 90 % decrease in melting times for a 0.05 vol fraction. Although nanoparticles can significantly improve the thermal conductivity of PCMs they are not as effective as fins when it comes to decreasing melting time. For the same displaced PCM volume fraction, fins alone perform better than nanoparticles as shown by Mahdi et al. [25] in their CFD analysis. Another drawback is that nanoparticles suppress natural and forced convection which is not beneficial for melting speed. This was studied using 2D simulations by Mohamad [26] showing that by adding nanoparticles to improve the thermal conductivity of the PCM, the natural convection is reduced. This is because of increased heat transfer from the upper liquid PCM to the lower liquid PCM which decreases the temperature difference and therefore the buoyancy force is also less. Aydin et al. [27] investigated the melting behaviour of a paraffin-based storage unit of the horizontal shell-and-tube heat exchanger. The different heights (10, 20, 30 and 40 mm) of fins under constant inlet temperature and mass flow rate of HTF. The results showed the maximum enhancement in melting rate of 72.8 % for the fin height of 40 mm compared to the without fin case. Alizadeh et al. [28] conducted a numerical study to investigate the latent heat thermal energy storage performance using nano PCM and hexagonal TTHX. Single wall carbon nanotubes are used as nanoparticles and copper made curved fins are integrated inside the TTHX. During the solidification process, it was found that optimized curved fins penetrated the intensity of energy storage into the PCM and solidification process was minimum due the high thermal performance of nanoparticles loadings and time perfection.

Fins provide a way to increase conduction within the PCM annulus by increasing the heat transfer area of the heat exchanger. Agyenium et al. [29] performed experimental studies using Erythritol PCM in heat exchangers with circular fins, longitudinal fins, and a control with no heat transfer enhancement. The results showed that longitudinal fins gave the best performance with better thermal performance when melting or solidifying the PCM. That is the reason why this type of fin will be used in this paper to optimise the melting process in TTHXs. A study on the use of fins to accelerate melting was conducted by Rathod et al. [30]. The study looked at heat transfer augmentation of PCM in a shell and tube heat exchanger using longitudinal fins in the heat transfer tube. The results of the study show that melting and solidification times can be reduced by up to 25.42 % and 43.6 % respectively. The study was not focused on optimising the configuration of these fins; however, it shows that fins can offer significant improvements in melting times. The geometry of the heat transfer fins has an impact on how effective they are at reducing the melt time of the PCM. Therefore, optimising the geometry of the fins is an important area of research and the subject of this paper.

Mahdi et al. [31] investigated novel fin configurations and found that they could reduce the melting time by up to 30 % when compared to a standard fin configuration. This shows that intelligent fin placement is very important. They also found that the differing melting mechanisms in the upper and lower half of the TTHX meant that a different fin configuration was needed for each half to optimise melting. Studies have shown that the buoyancy force is a major contributor to the melting process of PCMs. For example, Tiari et al. [32] the study found that natural convection led to a 30 % faster charging process and reduced the thermal resistance between the PCM melting front and the walls of the container. The container that was used in this study was square however similar conclusions are expected to apply to TTHXs. This shows that fin geometries should be designed to maximise natural convection. Ismail et al. [33] numerically and experimentally analysed the solidification of PCM around an axially finned cylinder which is similar to the case which will be investigated in this project. The results from the study show that the parameters which had the greatest effect were the fin length and the number of fins which is useful information when designing novel fin structures. Another study which used a different method to approach designing novel fin configurations and structures was Sciacovelli et al. [34]. Although the study was looking at optimising the solidification process of the PCM there will be some insights into how the melting process can be improved. Conduction is the most dominant form of heat transfer in the solidification process whereas in the melting process convection in the upper half and conduction in the lower half are the more dominant processes. The method used was a combination of CFD modelling [35] and the response surface method to enable the most optimal fin configuration to be found. Their study also was looking into the performance of Y-shaped fins, and they found that Y-shaped fins with wide angles between branches performed the best.

The novelty of this study can be summarised: a) We proposed a novel fin configuration to enhance the energy storage performance based on the liquid–solid interface evolution during the melting process of PCM-

based in tubular heat exchangers using transient simulations; b) The evolution of the fluid–solid interface of PCMS during melting process is described in detail considering the natural convection thanks to the buoyancy effects; and c) The optimisation of fin configurations is carried out to achieve high energy efficiency of PCM for the energy storage performance in tubular heat exchangers.

2. Problem statement

2.1. Physical model

The geometry for the TTHX was chosen to match the requirements of a liquid desiccant air-conditioning system because this is a common real-world use case. The TTHX consists of 3 tubes with the inner, middle, and outer tube diameters being 50.8 mm, 150 mm and 200 mm. The tube wall thickness for the middle and outer tubes is 2 mm and the inner tube wall thickness is 1.2 mm. The simplified geometry and layout of the TTHX and PCM domains are shown in Fig. 1 and Fig. 2.

Based on these dimensions the modelled geometry of the PCM domain consisted of two concentric circles with the $r_o = 73$ mm and the $r_i = 25.4$ mm. The annular space between the circles is where the PCM is, and the walls would be set at the temperature of the heat transfer fluid (HTF) which is generally water. The heat transfer fluid (HTF) is a fluid which transfers the heat into the PCM to melt or solidify it. In this case, the HTF will be hotter than the PCM's melting point to cause the PCM to melt. What the HTF is made up of does not make a difference to the simulation because it is assumed that the temperature of the walls is the same temperature as the HTF and the temperature of the HTF is constant. However, a common HTF for liquid desiccant air-conditioning systems is water. The walls and fins in contact with the PCM domain are made of copper due to their good thermal conductivity values and corrosion resistance. Table 1 shows the properties of RT82 which is the PCM material selected to simulate in this paper.

2.2. Governing equations

The main equations which govern the melting of the PCM are explained in this section. When the PCM is solid the main heat conduction mechanism is conduction however once the PCM begins to turn into liquid natural convection and conduction both occur. For the Fluent

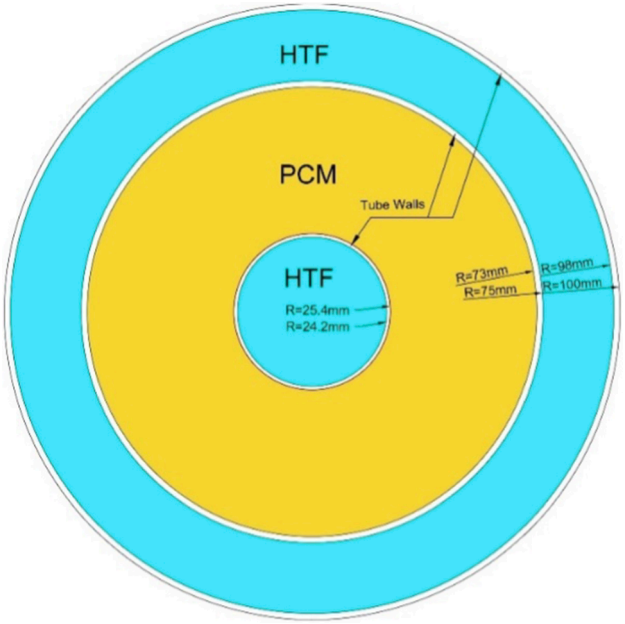

Fig. 1. Full TTHX geometry.

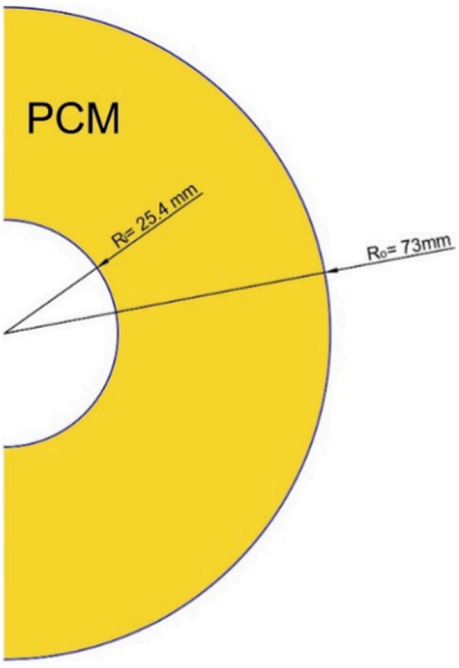

Fig. 2. Half of simple no fin geometry.

model the PCM flow is assumed to be laminar, transient, and incompressible as well as other assumptions detailed below [37]:

- At the walls are no-slip boundary conditions.
- The temperature change of the HTF is negligible therefore T_w = constant.
- The temperature change of the fins is negligible and therefore $T_F = T_{HTF}$.
- Viscous dissipations within the fluid are negligible.
- The thermophysical properties of the PCM are not affected by the temperature except the density in the momentum equations.
- Boussinesq approximation for density variation is valid for the case.
- Volume variation due to phase change is neglected.
- There is no heat loss or gain from the surroundings.

The Boussinesq approximation for density is used in the numerical simulations. It can be seen in equation (2) how it approximates density using the thermal expansion coefficient and the PCM material properties.

$$\rho = \rho_m(1 - \beta(T - T_m)) \tag{1}$$

where $\rho_m$is the density of the liquid PCM and T_m is defined as follows:

$$T_m = (T_s + T_l)/2 \tag{2}$$

where T_s and T_l are the solid and liquidus temperatures of RT82.

The main governing equations include the continuity equation as shown in equation (3), the energy equation for solidification and melting as shown below in equation (4) and the momentum equations as shown in equations (5) and (6). They govern the fluid motion and temperature distribution within the PCM.

$$\nabla \bullet V = 0 \tag{3}$$

$$\frac{\partial}{\partial t}(\rho H) + \nabla \bullet (\rho \vec{v} H) = \nabla \bullet (k \nabla T) + S \tag{4}$$

$$\frac{\partial u}{\partial t} + V \bullet \nabla u = \frac{1}{\rho}\left(-\nabla P + \mu \nabla^2 u\right) + S_u \tag{5}$$

Table 1
RT-82 PCM properties [36].

Properties	Values	Properties	Values	Properties	Values	Properties	Values
G (kJ/kg)	176	ρ (kg/m^3)	770	C_p (J/kg K)	2	k (W/m K)	0.2
μ (kg/ms)	0.03499	Ts (K)	350.15	T_l (K)	358.15	β (K^{-1})	0.001

$$\frac{\partial v}{\partial t} + V \bullet \nabla v = \frac{1}{\rho}\left(-\nabla P + \mu\nabla^2 v + \rho\beta g(T - T_{ref})\right) + S_v \tag{6}$$

$$S_u = -C(1-\lambda)^2 \frac{u}{\lambda^3 + \varepsilon} \tag{7}$$

$$S_v = -C(1-\lambda)^2 \frac{v}{\lambda^3 + \varepsilon} \tag{8}$$

where u and v are the components of velocity in the r and θ direction, μ is the dynamic viscosity, P is pressure and C is the mushy zone constant. The mushy zone constant controls the damping as velocity drops closer to zero when the PCM solidifies and was set to 10^5 due to it providing the closest match to the Al-Abidi et al. [38] experimental results. Also μ, ρ, β, k are the dynamic viscosity, density, thermal expansion coefficient, thermal conductivity respectively. The value ε in the equations (7) and (8) represents a small number around 0.001 used to avoid dividing by zero. The equation used to calculate the sensible enthalpy is equation (9).

$$h = h_{ref} + \int_{T_{ref}}^{T} C_p dT \tag{9}$$

where h is the sensible enthalpy and C_p is the heat capacity of the PCM.

The PCM can either be solid where the liquid fraction is 0, fully liquid where the liquid fraction is 1 or a mixture of both. The liquid fraction of the PCM denoted by λ is dependent on the temperature as can be seen by equation (10).

$$\lambda = \begin{cases} 0, T \le T_s \\ (T - T_s)/(T_l - T_s), T_s < T < T_l \\ 1, T \ge T_l \end{cases} \tag{10}$$

The energy stored in the PCM is dependent on how much of the PCM is a liquid and the PCM material heat of fusion. The latent heat stored in the PCM can be calculated using Equation (11) where ΔH is the latent heat and Γ is the heat of fusion.

$$\Delta H = \lambda\Gamma \tag{11}$$

2.3. Numerical implementation

The two-dimensional transient numerical simulations of PCM in a TTHX were carried out based on the commercial platform ANSYS Fluent-2020R1. The technique used to simulate the PCM melting was the enthalpy-porosity technique which tracks the liquid fraction of a cell rather than tracking the melting front [39]. The mushy zone is where the PCM is liquid and the solid is regarded as a porous zone with a porosity equal to the liquid fraction. This approach is valid because the porous enthalpy technique is used across all the domains, the PCM melting is laminar, transient and incompressible, Boussinesq equations are used for density change and the thermophysical characteristics of the PCM remain constant apart from the density change due to temperature change [15]. The mesh used in the simulation was a fixed mesh which means that the governing equations were modified for them to be correct for both phases. To discretise the governing equations the finite volume method (FVM) with higher order upstream interpolation for convective kinematics (QUICK) difference scheme was used. Then after the discretisation, a pressure-based method was used to solve the governing equations. A pressure-based solver is recommended for slow-moving incompressible fluids [40].

For the initial conditions, the temperatures of the inner and outer walls of the domain where the PCM is, are assumed to remain at a constant temperature of 363.15 K which is higher than the melting temperature of RT82 to cause it to heat up and melt. In addition, the PCM itself was given a starting temperature of 300.15 K as this is a value that all the PCM will be solid at. For the wall conditions, no-slip conditions were used in this simulation, which means that the walls of the annulus were set as copper material and the boundary condition was a nonslip condition.

3. Results and discussion

3.1. Model validation and validation

The number of cells used for the simple case with no fins was N = 25,724 as this was found to provide a good balance between accuracy and computing time. Fig. 3 shows the relationship between cell number and PCM liquid fraction over time. The difference between the three different mesh cell numbers is minimal which shows that at a cell number of 25,724 the solution is mesh independent. The timestep that was used was 0.1 s as provided a high resolution and was stable for all cases tested. The maximum iterations per timestep were set at 20 as this is the recommendation for most transient cases. Increasing the maximum number of iterations past 20 would not increase the accuracy noticeably and it would be more useful to have a smaller timestep than to increase the iterations per timestep. It was noted that other similar studies [31] used a timestep of 0.1 s which was also found to be stable. However, a timestep of 0.1 s was opted for due to the increased resolution. The under-relaxation factors for energy, pressure correction, and velocity components were set at 1, 0.3, and 0.5 respectively. The scales residuals using the formula shown in equation (12) to allow for convergence to be better judged. For the momentum equations the $a_P\Phi_P$ denominator is switched for $a_P v_P$ where v_P is the magnitude of velocity at cell P. For all equations R^Φ reduces to below 10^{-4} with some other equations such as energy reducing to below 10^{-6}.

$$R^\Phi = \frac{\sum_{cellsP}\left|\sum_{nb} a_{nb}\Phi_{nb} + b - a_P\Phi_P\right|}{\sum_{cellsP}\left|a_P\Phi_P\right|} \tag{12}$$

To validate the CFD model the experimental results from the Al-Abidi et al [38] were compared with the simulation results. The simulation was set up with similar boundary conditions, initial conditions and PCM material properties. Fig. 4 shows the comparison between experimental and numerical results of the average temperature of the PCM domain over time. Fig. 4 shows that the model closely follows the experimental results meaning that the model is validated experimentally.

3.2. Evolution of fluid–solid interface of PCM melting with no fins in TTHXs

The liquid fraction contour is the most useful figure when analysing the melting process of the PCM as it shows where the PCM is solid and liquid very clearly. A liquid fraction of 1 means that the PCM is a liquid and a value of 0 means the whole PCM is solid, liquid fraction values between 0 and 1 mean there is a mixture of liquid and solid PCM. The melting process in Fig. 5 is shown with liquid contours until 165 min. Fig. 6 shows the temperature of the PCM over time with the same time intervals as. There is a similar colour pattern to Fig. 5 because the PCM liquid fraction is dependent on the temperature. Fig. 7 shows the

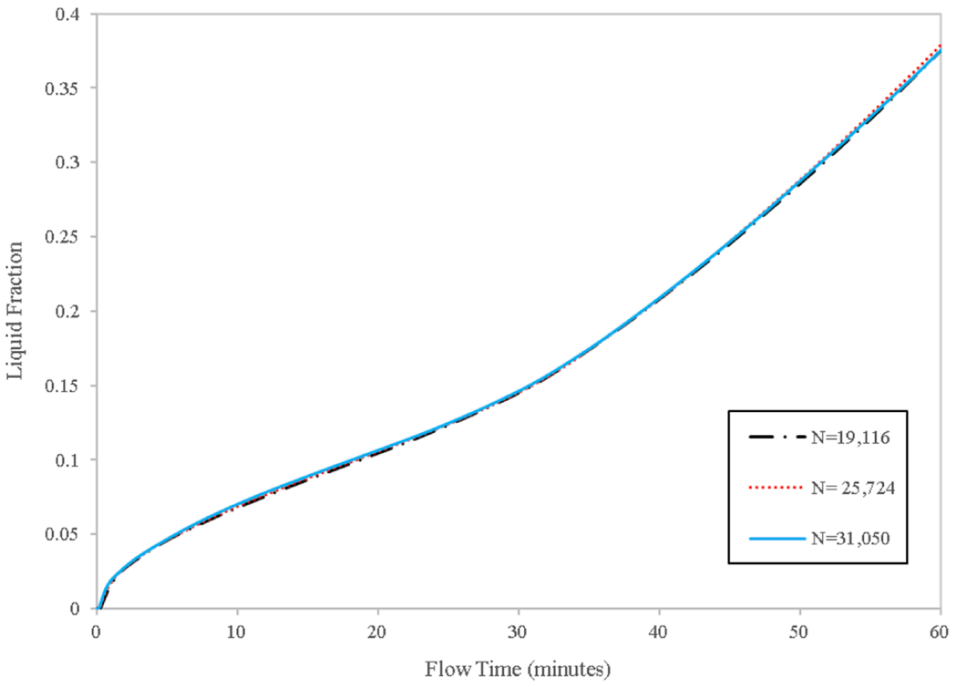

Fig. 3. Mesh independency study.

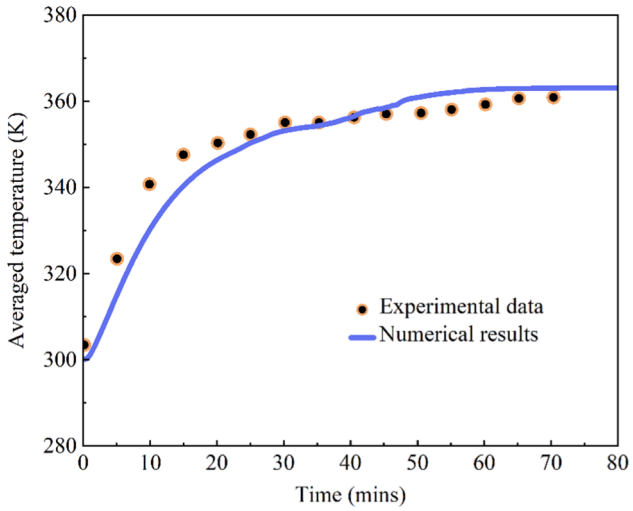

Fig. 4. Model validation of PCM melting process.

velocity vector during the melting process. Having information on the direction of the liquid PCM flow allows analysis of the convection behaviour in the melted PCM.

At the start of the melting process, after 15 min have passed, the main heat transfer mechanism throughout the domain is conduction as only a small percentage of the PCM is in the liquid phase. This can be shown by the thin layer of liquid fraction in Fig. 5 where there is very little convection. The small amount of convection occurring is shown by the velocity vectors in Fig. 7 which shows liquid PCM from around the outer tube wall of the TTHX, moving to the top. Another interesting pattern to note is that the melting pattern is largely the same in the upper and lower half as not enough PCM has melted yet to allow for natural convection to influence melting in the upper half of the TTHX. After around 45 min have passed small convection currents begin to form due to density variation in the liquid parts of the PCM. These convection currents are located on the bottom of the outer tube and the top of the inner tube. There is also a larger amount of liquid PCM in the upper annulus region which is due to convection currents carrying the hotter liquid PCM to the top of the TTHX further encouraging melting in the upper half.

The convection currents on the bottom of the outer tube and the top of the inner tube continue to grow as shown by the liquid fraction contour at 75 min in Fig. 5. However, the natural convection currents in the upper half of the PCM grow much more than in the lower half. This is because the hot liquid flows up from the bottom of the outer tube and the top of the inner tube. The result is a large proportion of the PCM in the upper half of the TTHX is now liquid and large convection currents are visible in this liquid PCM. At this point, it is clear that the upper half of the PCM is melting faster than the lower half. After 105 min the entire upper half of the PCM is fully liquid as Fig. 5 shows, whereas the lower half still has two solid PCM regions. This demonstrates that the upper half of the PCM melts considerably faster than the lower half of the PCM. This is because there are convection currents within the PCM which cause warmer liquid PCM to move to the upper half which accelerates the melting process. The currents are formed due to buoyancy forces caused by the PCM having a lower density at higher temperatures.

The convection currents are most visible in the 75 min liquid fraction contour in Fig. 5. Convection effects occur in the upper and lower half of the TTHX however they are less developed and contribute less to increasing the melting process in the lower half. Heat transfer and melting are more based on conduction in the lower half of the TTHX which is less effective and means the lower half takes longer to melt. By adding fins into the TTHX, especially in the lower half, heat transfer through conduction will increase due to the increased heat transfer area and the melting time of the PCM will shorten. The non-uniform melting in the simple no fin geometry is not conducive to efficient energy storage and therefore requires optimisation which is what is the aim of this study.

3.3. Optimisation of fin configurations for enhancing PCM thermal energy storage

3.3.1. Concepts for fin configurations based on fluid–solid interfaces of PCM

Fig. 8 shows five concept geometries of fin configurations based on

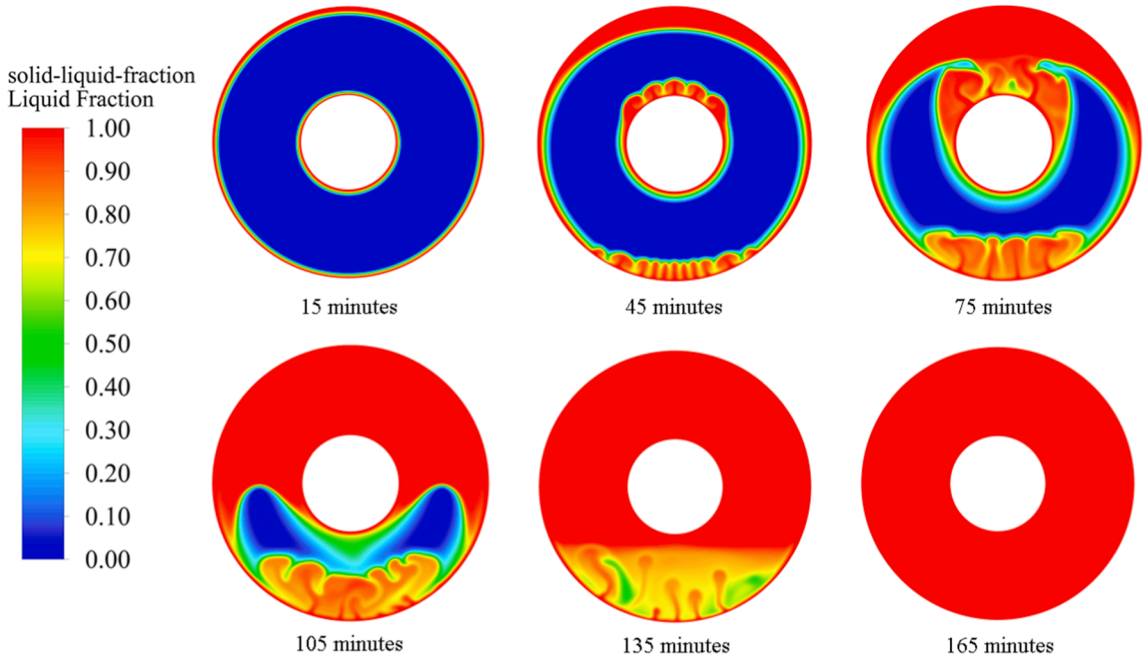

Fig. 5. Contours of liquid fraction at various times through the melting process.

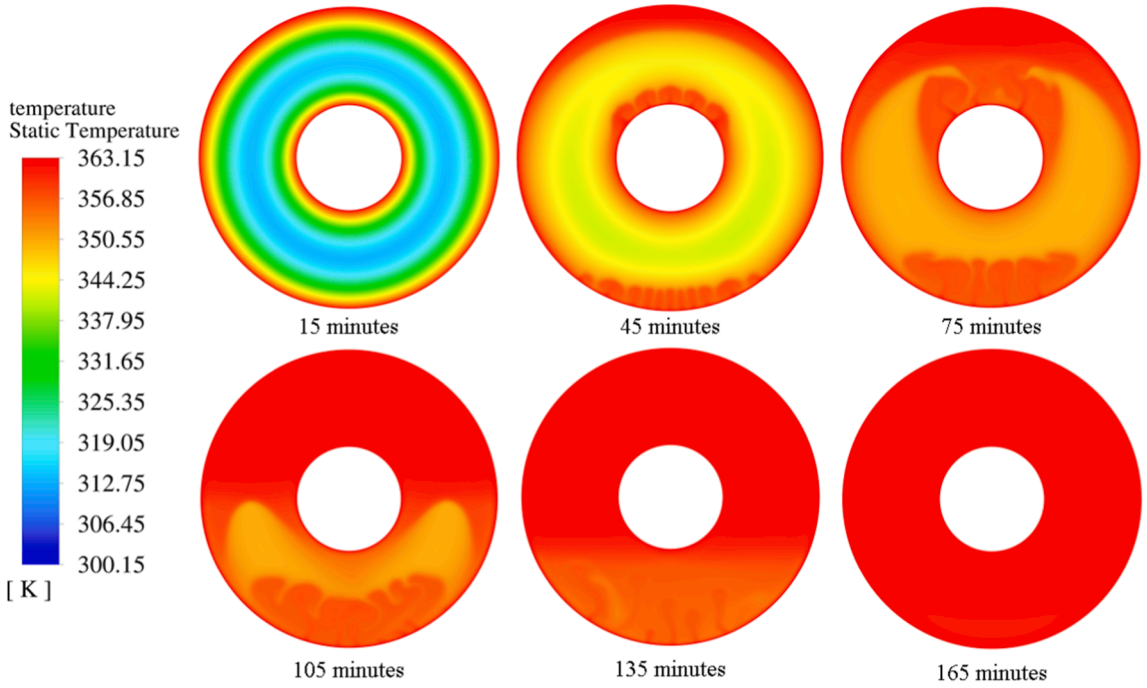

Fig. 6. Temperature contours at various times through the melting process.

fluid–solid interfaces during the melting process of PCM, which are primarily designed to combat the slower melting in the lower half of the TTHX through fins to improve conductive heat transfer and to encourage convection in the upper half. The aim is to shorten the time it takes to fully melt the PCM and therefore improve the heat storage rate. All geometries apart from concept 3 are designed to place fins in the location where the PCM remains solid the longest in melting. By adding fins in these areas, the solid PCM there will melt faster, and the total melt time will in theory decrease. Concept 3 was an experimental case to explore the effect of fins limiting natural convection and therefore should not be expected to outperform the other concepts. The details of all cases with reasonings have been mentioned in Table 2.

The location and shape of the fins were designed not to limit the contribution of natural convection which is an important heat transfer mechanism. Various approaches were taken with the fin geometries to try and find what features accelerate the melting the most. The fin volume fraction was kept as a small percentage of the total volume to reduce the amount of the PCM that is displaced. A low fin width of 1 mm was used for all fin concepts as this reduced fin volume fraction while still retaining structural strength. Maintaining a low fin volume fraction is important because if there is less PCM in the TTHX then less heat can be stored. Therefore, the fin volume fraction only made up at most 1.6 %

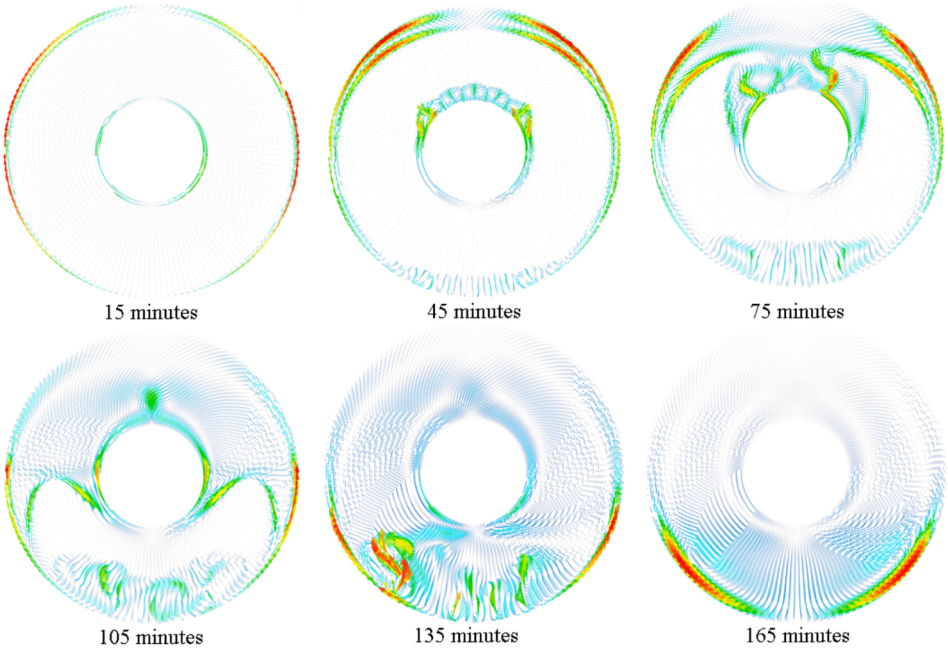

(a) Melting process from 15 mins to 165 mins

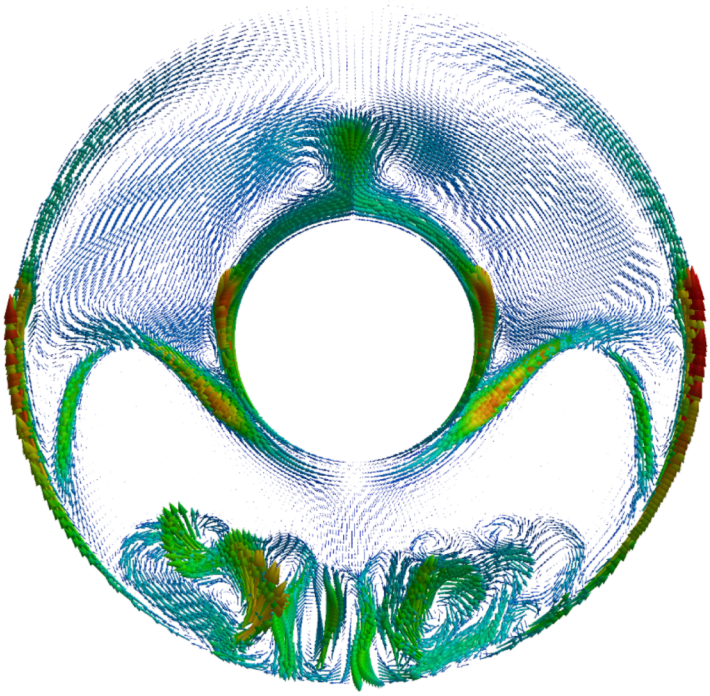

(b) Detailed velocity vectors at 105 mins

Fig. 7. Velocity vector plot at various times through the melting process.

of the total volume (as shown in Table 3) which is meant that the change in PCM volume is negligible. In addition, the fin volume variation between each concept was intentionally kept as small as possible to eliminate the effect of different fin volumes. This allowed a more accurate comparison between each of the concepts. The fin geometries were created by removing the PCM area where the fins would be and setting the new walls at the HTF temperature the same way the normal tube walls touching the HTF were set up. Therefore, to calculate the fin volume and the surface area (S.A.) of the fins, the geometries were calculated in Ansys-Fluent and compared to the simple case surface using Equation (13).

$$Finvolumefraction = \frac{SimplecaseS.A. - FinCaseS.A.}{SimplecaseS.A.} \tag{13}$$

3.3.2. Optimisation results

The melting behaviour of fin concepts after 20 min is similar to the pattern displayed in all the fin cases with layers of liquid PCM gathered along the walls and fins of the TTHX. This can be seen in Fig. 9 which

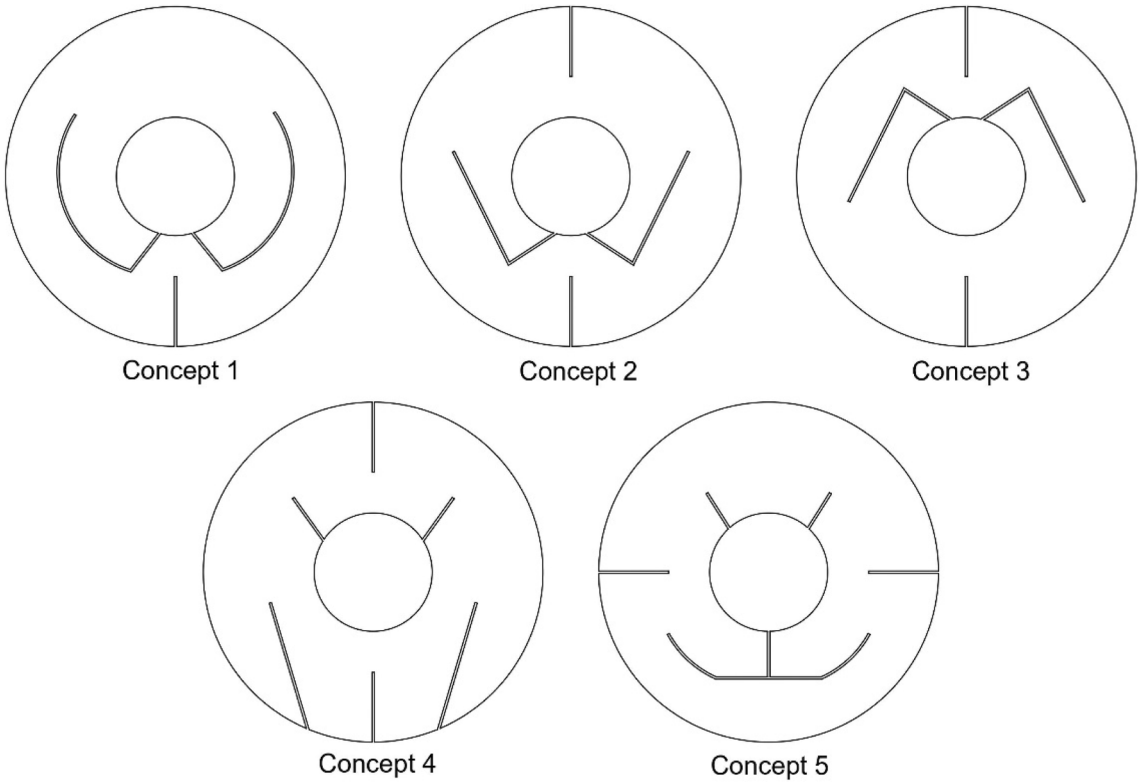

Fig. 8. Concepts for fin configurations based on fluid–solid interfaces during melting process of PCM.

Table 2
The configuration of all cases used in the current study.

Concept	Unique Design Idea
1	• Place curved fins in the areas where the PCM melted last in the simple case. • The idea of curved fins was to allow for a smooth flow of melted PCM into the upper half thereby increasing the natural convection effect.
2	• A variation of concept 1 with straight fins allowed an extra fin to be added into the upper half due to straight lines having a shorter length when compared to arcs. • The aim was to see whether the curved fins were important and whether straight fins were comparable.
3	• This concept aimed to test the idea that upside-down angled fins reduce natural convection and therefore slow down the melting process. • Not designed to be the fastest melting case, rather it was made to study the movement of the melted PCM.
4	• In this concept, the fins were straight and attached to the lower surface of the outer tube. This was to try and prevent any melted PCM from getting trapped under the inner tube where natural convection could not occur. • The fins till were also designed to be passing through the region where the PCM remained solid for the longest in the simple case. • The fins were also very vertical which is the opposite theory compared to case 5 which had as many horizontal surfaces as possible.
5	• After being inspired by the research by Kamkari et al. [41] and Yan et al. [42], concept 5 was designed to have many horizontal surfaces. This is because the paper suggested that vertical walls are not as effective as angled or horizontal walls at transferring heat and encouraging natural convection. The reason why this occurred was that the liquid layer became stratified when the wall was vertical which slowed down the heat transfer into the. • The idea was to maximise both conduction and convection in the lower half of the PCM by adding horizontal fin surfaces to speed up the melting time.

Table 3
Fin volume fractions for various concepts.

Concept No.	Fin Volume Fraction	Fin Volume Percentage
1	0.0160	1.60 %
2	0.0146	1.46 %
3	0.0146	1.46 %
4	0.0148	1.48 %
5	0.0147	1.47 %

shows the liquid fraction at 20 min. The difference between the fin and no fin cases is that the layer of liquid PCM is thicker in some places such as beneath the inner tube and at the fin tips than in the no fin case. At this stage in the melting process, conduction is the primary melting mechanism as not enough PCM is liquid for natural convection currents to develop. Greater amounts of liquid PCM at the fin tips suggest that the extra heat-exchange area that the fins provide, quickens the onset of natural convection. Evidence of earlier natural convection can also be seen in Fig. 9 by the larger convection currents compared to the non-fin case at the bottom of the PCM annulus in all fin concepts due to the fins increasing heat transfer in that region.

After 40 min have passed convection currents in all fin cases can be seen in Fig. 9 and deforming the liquid–solid contour. These convection currents are pronounced in all concepts apart from concept 3 which has fewer convection currents in the upper half. This is due to the fact that most of the upper half of concept 3 has melted after 40 min and the fins in the annulus are limiting convection from the lower half. The fin cases after 40 min have melted around 60–70 % of the PCM compared to the no fin case which only melted 20 % of the PCM in that time frame. This shows effective melting acceleration in the early stages. The spread of solid PCM in the TTHX after 40 min is different for each fin concept. In concepts 1 and 5 most of the solid PCM is in the upper half, in concepts 2 and 4 there is an even spread and concept 3 has the most solid PCM in the lower half. One cause of concepts 1 and 5 having more solid PCM in the upper half compared to concepts 2 and 4 is the lack of a vertical fin at the top of the outer tube. From the liquid fraction contours in Fig. 9, it can be seen that concepts with the vertical fin there see faster melting in that region. Concepts 1 and 5 have a higher proportion of their fins in the

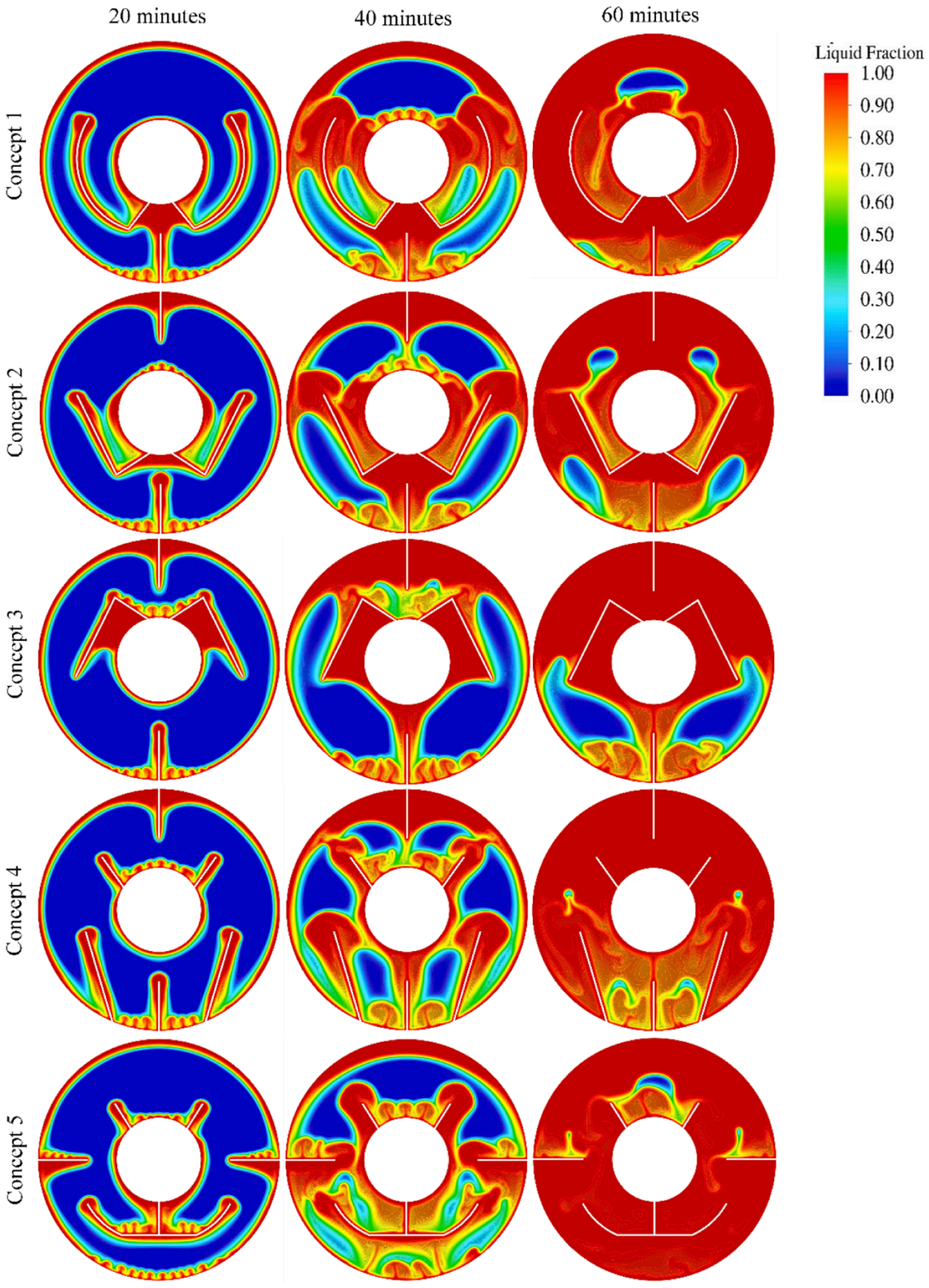

Fig. 9. Liquid fraction contours for fin concepts.

lower half which explains why that region has melted faster than the upper half. The other key point to note after 40 min in Fig. 9 the lower half of concept 5 is mostly liquid which shows that the melting acceleration in that region is successful. Other concepts do not have as much of the lower half melted at this point and later this results in a slower full melt time. This is because melting the lower half is much slower than in the upper half due to less natural convection and reliance on conduction for heat transfer. After 60 min of melting, the vast majority of the PCM in the TTHX is liquid with only a few isolated spots with solid PCM. The liquid fraction in Fig. 9 shows that concepts 4 and 5 have the highest liquid fraction and therefore most effective at melting PCM after 60 min.

Fin concepts 1 and 2 were designed to look very similar in terms of

fin geometry however concept 2 took almost 8 min longer than concept 1 to fully melt as shown in Fig. 9. This is interesting because the small differences between the concepts are the fins attached to the inner tubes are arcs in concept 1 and straight in concept 2, as well as concept 2 has an extra vertical fin in the upper half of the annulus. This shows that small geometry differences can have a measurable effect on melting time. The extra fin in the upper half of the annulus in concept 2 can be seen in Fig. 9 to have a beneficial effect in accelerating the melting process in that region. However, the straight fins in the lower half of the PCM do not provide the same level of accelerated melting effect as the

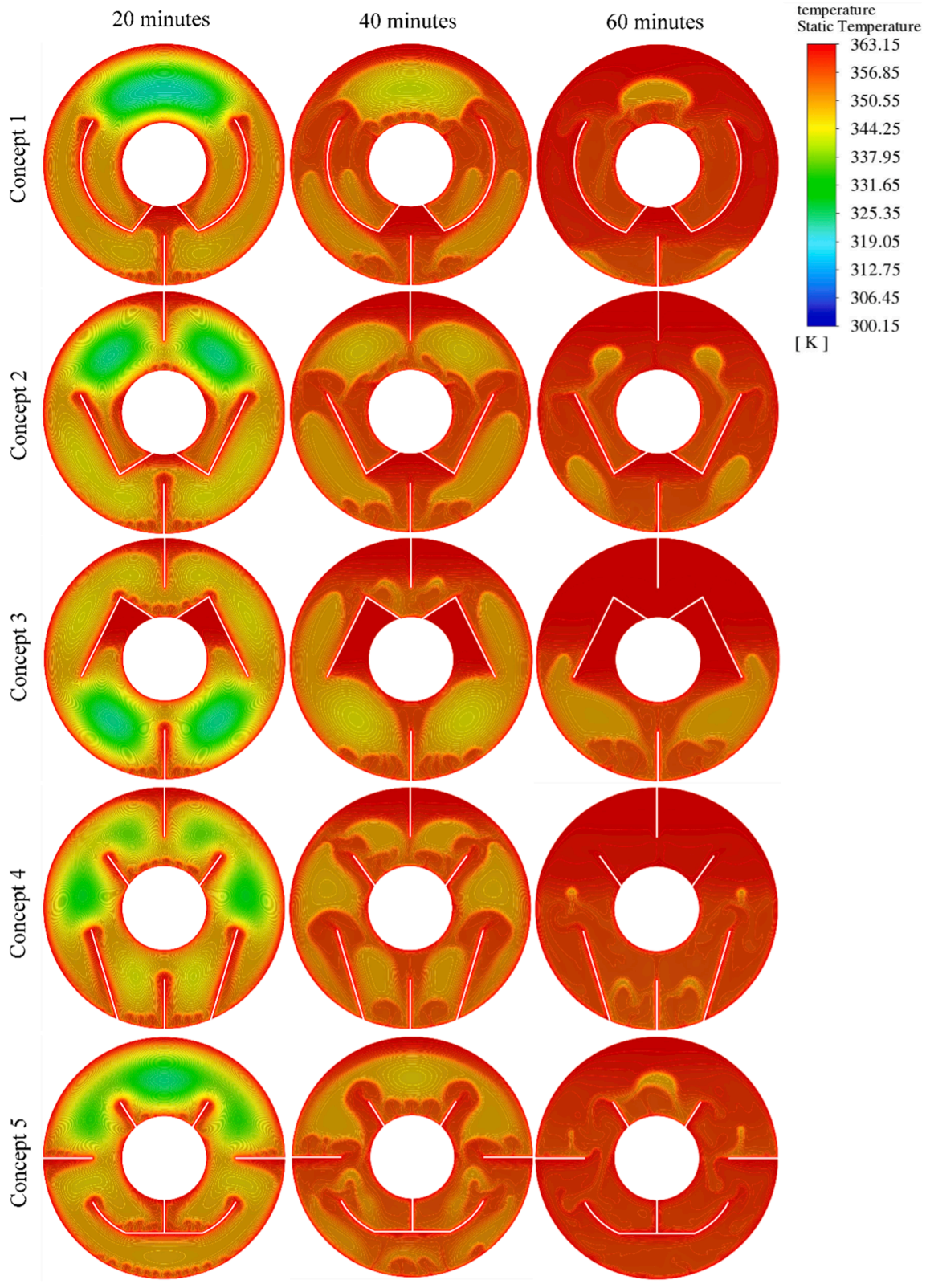

Fig. 10. Temperature contours for fin concepts.

curved fins in concept 1. As a result, it can be seen in Fig. 9 that concept 2 has much more solid PCM in the lower half after 40 min when compared to concept 1 at the same point. This can be explained by the curved fins reaching more solid PCM in the lower half due to their curved shape and a longer length which better fits the circular TTHX design. The curved fins better reaching the PCM in the circular TTHX is much more likely the reason why concept 1 melted faster than concept 2 and not the fact that curved fins allow for a smoother flow of liquid PCM. For that theory to work the velocity of the natural convection currents would have to be much higher than the velocity was.

Fig. 10 shows the isothermal contours of the fin concepts over time. At 20 min the temperature contour shows the areas with the lowest temperature and the lowest isothermal contour density. These regions are the hardest to heat up for the PCM and tend to be the slowest to melt. All concepts apart from concept 5 have areas of lower temperature in the lower half after 20 min. This foreshadows the faster melting time that concept 5 achieves. After 40 min the temperature contour shows isothermal lines which have deformed away from the fin and walls that they are usually parallel to. This shows convection currents and rotational flows as more PCM becomes liquid as temperatures rise. The concept 4 contour shows the lowest number of convection currents which is partly due to the fins reducing convection by trapping flows, as shown in Fig. 10. On the other hand, concept 5 has the greatest number of convection currents suggesting that the melting time will be accelerated. In the 60 min contours 1, 4 and 5 show the highest average temperatures and the isothermal contours are very deformed showing that convection currents are fully developed. By this stage, most of the PCM is the same temperature with only a few hard-to-reach areas remaining cooler than average.

The average liquid fraction over the domain was reported for each timestep as shown in Figs. 11–13. This allowed the melt times to be compared with a high resolution and the final melt times compared. The red dashed vertical lines with labels in Fig. 11 show the time taken for each concept to fully melt the PCM in the domain. The graph shows that early in the melting process from 0 to 39 min, concept 2 has a higher liquid fraction than concept 1. However, after 39 min concept 1 outperforms concept 2. The initial gradient of concept 2 is greater than the gradient of concept 1 but after the initial spike in a liquid fraction the slightly higher long-term gradient of concept 1 results in concept 1 fully melting the PCM 8 min before concept 2 does. This is due to the vertical fin in the upper half of concept 2 melting the PCM in the upper region faster initially compared to concept 1 which does not have a fin in that area. After 39 min when improved conduction in the lower half was more important than greater heat conduction in the upper half concept 1 had an advantage over concept 2 and melted faster overall. A common feature in the liquid fraction contours of all fin concepts (shown in Fig. 9) is that where there is a vertical fin attached to the top of the outer tube, natural convection is increased on the inner tube's upper surface. This is due to the increased heat transfer that the fin provides to that region. It is an important feature because natural convection accelerates melting and it shows that the fin there does not just increase conduction in the PCM but also improves convection noticeably.

Concept 3 had the exact same geometry as concept 2 but was rotated 180 degrees to see how the natural convection effects are changed, as shown in Fig. 12. The results show that early on until around 25 min have passed the average liquid fraction of concept 3 is not noticeably different when compared to other cases. Only after 25 min when most of the PCM in the upper half of the PCM has melted does the melting rate slow down as the lack of fins in the lower half of the PCM causes melting there to occur slower. The final melt time of concept 3 was 98 min which is much longer than the other fin geometries. This highlights the importance of adding fins into the lower half of the PCM and that the total melting time is closely linked to how fast the lower half of the PCM melts as this region melts the slowest naturally. Fig. 12 shows that Concept 4 achieved the fastest rate of melting out of all the concepts in the early stages up until 40 min after which concept 5 had a higher liquid fraction and fully melted faster. The early success could be credited to the higher fin volume fraction in the upper half of the PCM which lost its effectiveness after most of the PCM in the upper half had melted and the fins would have been better placed lower in the PCM annulus.

Concept 5 was the best concept as it accelerated the melt time the most reducing it from 155 to 66 min (57.4 % reduction), as shown in Fig. 13. There are a few reasons that explain why the concept performance exceeded the other concepts. The first and possibly the most important factor was that the concept had the highest fraction of fins in the lower half with 84 % of the fins being located there. This meant that by 40 min the lower region of the PCM was almost entirely melted leaving only the upper region to melt which it did 26 min later. The

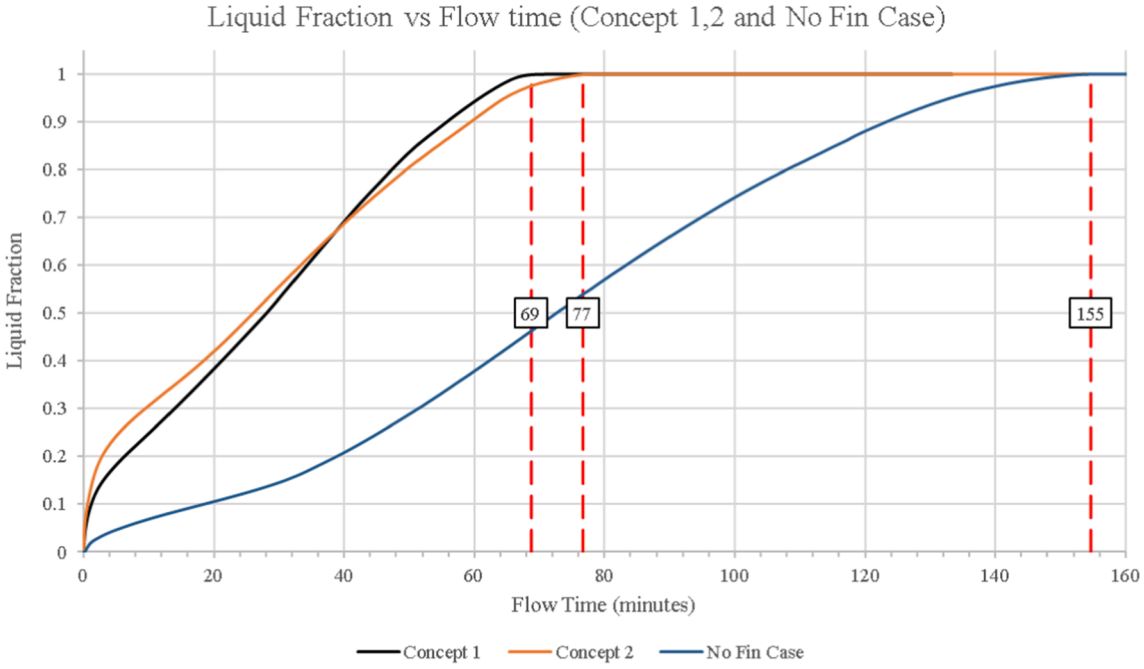

Fig. 11. Fin concepts 1, 2 and no fin case for liquid fraction over time.

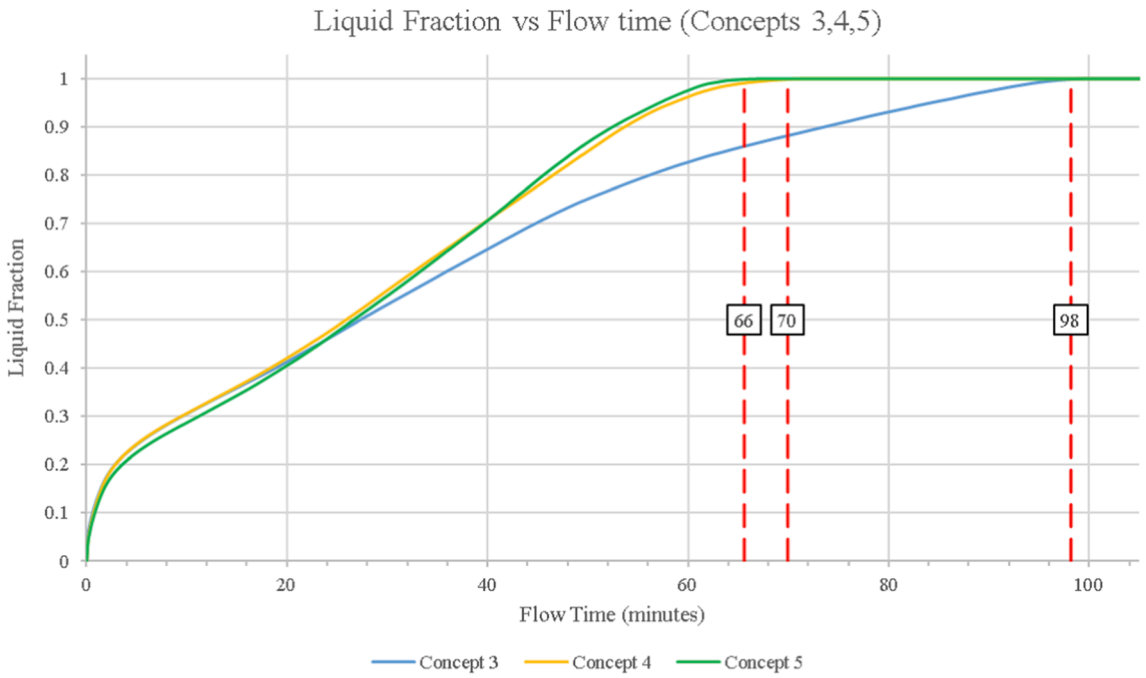

Fig. 12. Fin Concepts 3–5 for liquid fraction over time.

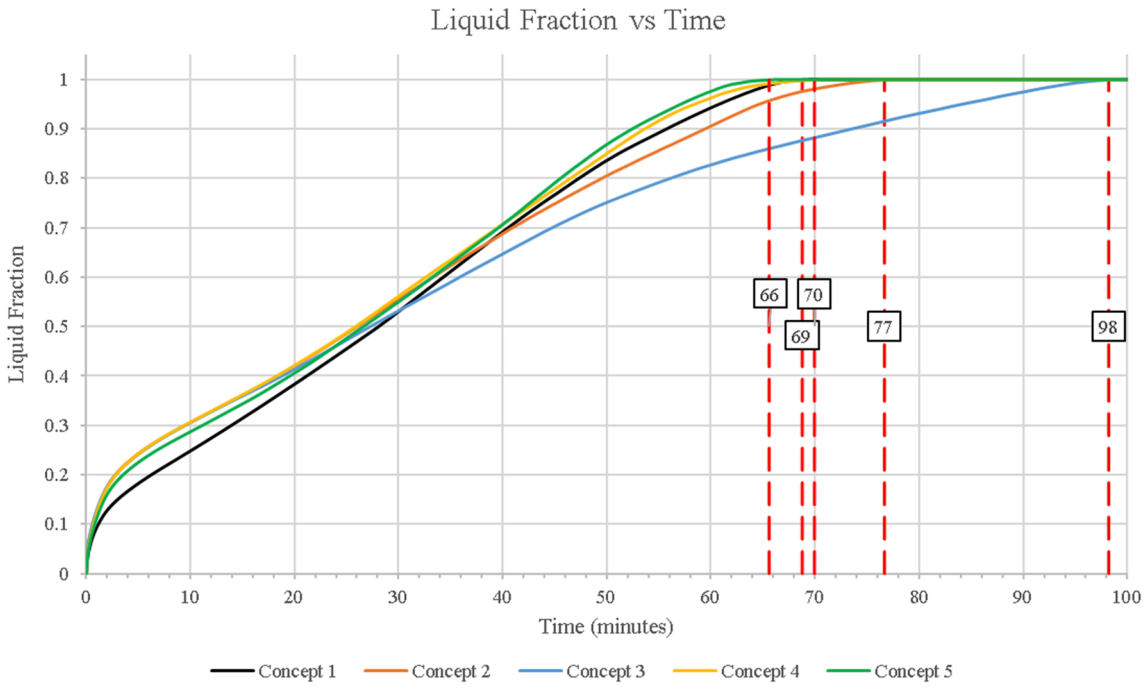

Fig. 13. Improved thermal energy storage of PCM including all the concepts.

theory behind concept 5 was to include as many horizontal surfaces as possible through the addition of fins to maximise natural convection. This theory appeared to be successful as can be seen in Fig. 9 by the 20-minute liquid fraction contour for concept 5 by the deformed liquid fraction fronts above the horizontal fin surfaces. Another small factor that also may have contributed to the exceptional performance of concept 5 was the curved fin tips of the inverted *t*-shaped fin in the lower half of the PCM. As concept 1 showed the curved fins better reach PCM and this could have given the same advantage to concept 5 as well.

Fig. 14 shows that the improvement from adding fins into the PCM annulus is dramatic even when the displaced volume of PCM is only 1.5 %. Concept 5 demonstrated the greatest improvement out of all fin concepts in full melt time with a 57.4 % reduction in time. This is comparable to other studies such as Mahdi et al. [25] which found that the fin case resulted in a 59.2 % time saving compared to the no fin case. Also, in another study Mahdi et al. [31] found a 63 % time-saving in PCM melt time when using a novel fin structure. In both studies, the fin volume fraction was 2 % compared to the 1.5 % volume fraction used in this project which could explain the slightly better results that were achieved.

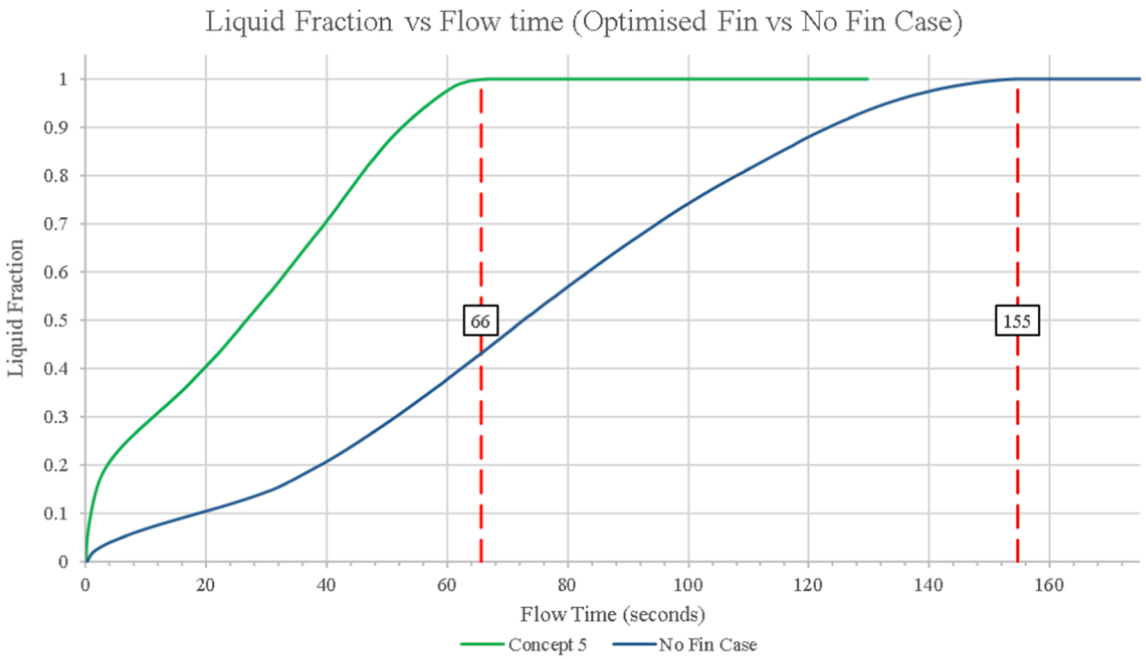

Fig. 14. Liquid fraction vs time graph of concept 5 and the no fin case.

3.4. Discussion

Numerical studies are carried out to understand the melting process of phase change materials for the thermal energy storage units in solar-based heating and cooling systems. The developed numerical method is validated against experimental data to demonstrate the accuracy of the computational model. The experimental studies will be an advantage to the numerical evaluation of the performance of phase change material. On the one hand, it will be very useful to use the experimental study to further validate the numerical model, which will improve the understanding how the accuracy of the developed model in the prediction of the transient flow and heat transfer behaviour in the melting process of PCM. On the other hand, experimental studies could be employed to evaluate the effect of different types of fin configurations on the PCM melting process. This will also demonstrate how the optimised fin configurations can contribute to enhanced heat transfer for phase change materials.

The future work includes a) The charging process and discharging process are both very important for the performance evaluation of phase change materials. In the next step, we will try to figure out the mechanism of the solidification process of phase change materials and how the discharging process can affect the thermal energy storage performance; b) The experimental studies are significant to understand the performance of phase change materials. It is expected to carry out experimental measurements on the melting process and solidification process of phase change materials which will not only be used to validate the numerical model but also will be useful to reveal the convection behaviour during the charging process of PCM; and c) The evaluation of the system energy efficiency is expected to be performed to assess how the integration of the thermal energy storage unit using phase change materials can contribute to the solar-based heating and cooling system.

4. Conclusions

The melting phenomenon of novel triplex-tube heat exchangers (TTHXs) was evaluated in current studies with different design concepts of fins integrated with PCM. The standard no-fin PCM annulus was simulated and analysed to see where fins should be placed. The analysis showed that the melting rates in the upper and lower half of the PCM varied considerably with the lower half taking much longer to melt fully. As a result of this finding, various fin concepts were created to try and accelerate the melting of the PCM focusing mostly on increasing the melting rate in the lower half. The full melt time of the PCM is important because if the PCM TTHX is used in an energy storage application in a shorter time. This is the reason why the full melt time of the fin concepts was used to measure success. The most successful fin concept was concept 5 and this will be compared to the no fin simple case in this section. There were several important findings related to the impact of fins on the melting of PCM in TTHX which will hopefully inform further research on the subject.

- Firstly, curved fins are superior when compared to straight fins due to their better fit with the circular tubed TTHX as evidenced by comparing concepts 1 and 2. This is a novel finding that has not been explored by other papers and required further study and experimentation to fully understand.
- Secondly, the importance of adding a higher proportion of fins to the lower half of the PCM was reinforced by concept 5 which had the highest proportion of fins in the lower half and performed the best. The relationship between the proportion of fins in the lower half and melt time is generally true however it is not perfect and concept 4 outperformed concept 2 despite concept 2 having a higher proportion of fins in the lower half.
- Thirdly, the experiment in concept 5 with adding many horizontal fin surfaces to the TTHX proved to be successful with that concept achieving the lowest full melting time with a value of 66 min. This shows that the report from Kamkari et al. [41] that natural convection is greatest on horizontal or angled surfaces in a rectangular container is also applicable to circular PCM TTHX. This idea has not been explored previously by other papers explicitly.

CRediT authorship contribution statement

Ben Palmer: Investigation, Discussion, Writing - original draft preparation and Revising. **Adeel Arshad:** Discussion, Reviewing and Revising. **Yan Yang:** Conceptualization, Methodology, Validation, Reviewing and Revising. **Chuang Wen:** Supervision, Conceptualization, Methodology, Investigation, Reviewing and Revising.

Declaration of Competing Interest

The authors declare that they have no known competing financial interests or personal relationships that could have appeared to influence the work reported in this paper.

Data availability

The research data supporting this publication are provided within this paper.

References

[1] Wu D, Rahim M, El Ganaoui M, Bennacer R, Liu B. Multilayer assembly of phase change material and bio-based concrete: a passive envelope to improve the energy and hygrothermal performance of buildings. Energ Conver Manage 2022;257:115454.

[2] Zhang J, Cao Z, Huang S, Huang X, Liang K, Yang Y, et al. Improving the melting performance of phase change materials using novel fins and nanoparticles in tubular energy storage systems. Appl Energy 2022;322:119416.

[3] Arshad A, Jabbal M, Yan Y, Darkwa J. The micro-/nano-PCMs for thermal energy storage systems: a state of art review. Int J Energy Res 2019;43:5572–620.

[4] Nejat P, Jomehzadeh F, Taheri MM, Gohari M, Abd. Majid MZ. A global review of energy consumption, CO2 emissions and policy in the residential sector (with an overview of the top ten CO2 emitting countries). Renew Sustain Energy Rev 2015;43:843–62.

[5] Daneshazarian R, Bayomy AM, Dworkin SB. NanoPCM based thermal energy storage system for a residential building. Energ Conver Manage 2022;254:115208.

[6] Kishore RA, Bianchi MV, Booten C, Vidal J, Jackson R. Enhancing building energy performance by effectively using phase change material and dynamic insulation in walls. Appl Energy 2021;283:116306.

[7] Han Y, Yang Y, Mallick T, Wen C. Nanoparticles to enhance melting performance of phase change materials for thermal energy storage. Nanomaterials 2022:12.

[8] Al-Yasiri Q, Szabó M. Energetic and thermal comfort assessment of phase change material passively incorporated building envelope in severe hot Climate: an experimental study. Appl Energy 2022;314:118957.

[9] Hlanze P, Elhefny A, Jiang Z, Cai J, Shabgard H. In-duct phase change material-based energy storage to enhance building demand flexibility. Appl Energy 2022;310:118520.

[10] Faraji H, El Alami M, Arshad A, Faraji M. Numerical simulation of the melting of a NePCM for cooling of electronic components. Therm Sci Eng Prog 2021;21:100766.

[11] Pandey K, Ali SF, Gupta SK, Saikia P, Rakshit D, Saha S. Facile technique to encapsulate phase change material in an amphiphilic polymeric matrix for thermal energy storage. Appl Energy 2021;292:116917.

[12] Yang W, Zhou F, Chen X, Zhang Y. Performance analysis of axial air cooling system with shark-skin bionic structure containing phase change material. Energ Conver Manage 2021;250:114921.

[13] Sun X, Lin Y, Zhu Z, Li J. Optimized design of a distributed photovoltaic system in a building with phase change materials. Appl Energy 2022;306:118010.

[14] Yazici MY. The effect of a new design preheating unit integrated to graphite matrix composite with phase change battery thermal management in low-temperature environment: an experimental study. Therm Sci Eng Prog 2022;29:101244.

[15] Arshad A, Jabbal M, Faraji H, Talebizadehsardari P, Bashir MA, Yan Y. Thermal performance of a phase change material-based heat sink in presence of nanoparticles and metal-foam to enhance cooling performance of electronics. J Storage Mater 2022;48:103882.

[16] [16] Arshad A, Faraji H, Jabbal M, Yan Y. A numerical study of HNCPCM filled metal-foam strips based heat sink for passive cooling. In: 2021 20th IEEE Intersociety Conference on Thermal and Thermomechanical Phenomena in Electronic Systems (iTherm); 2021. p. 524–30.

[17] Arshad A, Jabbal M, Shi L, Yan Y. Thermophysical characteristics and enhancement analysis of carbon-additives phase change mono and hybrid materials for thermal management of electronic devices. J Storage Mater 2021;34:102231.

[18] Yazdanifard F, Ameri M, Taylor R. Parametric investigation of a nanofluid-NEPCM based spectral splitting photovoltaic/thermal system. Energ Conver Manage 2021;240:114232.

[19] Arshad A, Jabbal M, Yan Y. Preparation and characteristics evaluation of mono and hybrid nano-enhanced phase change materials (NePCMs) for thermal management of microelectronics. Energ Conver Manage 2020;205:112444.

[20] Ali HM, Arshad A, Jabbal M, Verdin PG. Thermal management of electronics devices with PCMs filled pin-fin heat sinks: a comparison. Int J Heat Mass Transf 2018;117:1199–204.

[21] Kant K, Pitchumani R. Analysis of a novel constructal fin tree embedded thermochemical energy storage for buildings applications. Energ Conver Manage 2022;258:115542.

[22] Arshad A, Ibrahim Alabdullatif M, Jabbal M, Yan Y. Towards the thermal management of electronic devices: a parametric investigation of finned heat sink filled with PCM. Int Commun Heat Mass Transfer 2021;129:105643.

[23] Khodadadi JM, Hosseinizadeh SF. Nanoparticle-enhanced phase change materials (NEPCM) with great potential for improved thermal energy storage. Int Commun Heat Mass Transfer 2007;34:534–43.

[24] Jasim M, Mahdi ECN. Melting enhancement in triplex-tube latent heat energy storage system using nanoparticles-metal foam combination. Appl Energy 2017;191:31.

[25] Jasim M, Mahdi ECN. Melting enhancement in triplex-tube latent thermal energy storage system using nanoparticles-fins combination. Int J Heat Mass Transf 2017;109:426.

[26] Mohamad AA. Myth about nano-fluid heat transfer enhancement. Int J Heat Mass Transf 2015;86:397–403.

[27] Aydin O, Mete A, Yazici MY, Akgun M. Enhancing storage performance in a tube-in shell storage unit by attaching a conducting fin to the bottom of the tube. Isı Bilimi ve Tekniği Dergisi 2018;38:1–13.

[28] Alizadeh M, Haq RU, Hamid M, Nguyen VB, Truong TH, Ganji DD, et al. An analysis of latent heat thermal energy storage in a hexagonal triplex-tube unit with curve shape fin and CNTs. Case Stud Therm Eng 2022;36:102241.

[29] Agyenim F, Eames P, Smyth M. A comparison of heat transfer enhancement in a medium temperature thermal energy storage heat exchanger using fins. Sol Energy 2009:1509–20.

[30] Rathod MK, Banerjee J. Thermal performance enhancement of shell and tube Latent Heat Storage Unit using longitudinal fins. Appl Therm Eng 2015;75:1084–92.

[31] Jasim M, Mahdi SL, Ganji DD, Nsofor EC. Accelerated melting of PCM in energy storage systems via novel configuration of fins in the triplex-tube heat exchanger. Int J Heat Mass Transf 2018;124:663–76.

[32] Tiari S, Qiu S, Mahdavi M. Numerical study of finned heat pipe-assisted thermal energy storage system with high temperature phase change material. Energ Conver Manage 2015;89:833–42.

[33] Ismail KAR, Alvies CLF, Modesto MS. Numerical and experimental study on the solidification of PCM around a vertical axially finned isothermal cylinder. Appl Therm Eng 2001;21:53–77.

[34] Sciacovelli A, Gagliardi F, Verda V. Maximization of performance of a PCM latent heat storage system with innovative fins. Appl Energy 2015;137:707–15.

[35] Leong KY, Hasbi S, Gurunathan BA. State of art review on the solidification and melting characteristics of phase change material in triplex-tube thermal energy storage. J Storage Mater 2021:41.

[36] Al-Mudhafara AHN, Nowakowskib AF, Nicolleau FCGA. Enhancing the thermal performance of PCM in a shell and tube latentheat energy storage system by utilizing innovative fins. Elsevier; 2021.

[37] Arshad A, Jabbal M, Sardari PT, Bashir MA, Faraji H, Yan Y. Transient simulation of finned heat sinks embedded with PCM for electronics cooling. Therm Sci Eng Prog 2020;18:100520.

[38] Abduljalil A, Al-Abidi SM, Sopian K, Sulaiman MY, Mohammad ATh. Experimental study of melting and solidification of PCM in a triplex tube heat exchanger with fins. Energ Build 2014;68(Part A):33–41.

[39] Qaiser R, Khan MM, Ahmed HF, Malik FK, Irfan M, Ahad IU. Performance enhancement of latent energy storage system using effective designs of tubes and shell. Energy Rep 2022;8:3856–72.

[40] Ghalambaz M, Mohammed HI, Mahdi JM, Eisapour AH, Younis O, Ghosh A, et al. Intensifying the charging response of a phase-change material with twisted fin arrays in a shell-and-tube storage system. Energies 2021:14.

[41] Kamkari B, Shokouhmand H, Bruno F. Experimental investigation of the effect of inclination angle on convection-driven melting of phase change material in a rectangular enclosure. Int J Heat Mass Transf 2014;72:186–200.

[42] Yan P, Fan W, Yang Y, Ding H, Arshad A, Wen C. Performance enhancement of phase change materials in triplex-tube latent heat energy storage system using novel fin configurations. Appl Energy 2022;327:120064.